PROCEEDINGS of the
24th International Congress on Acoustics

October 24 to 28, 2022 in Gyeongju, Korea

ABS-0618

Acoustic characterization of impacted rectangular plates

Martin Czuka(1), Marian Weger(2), Robert Höldrich(2)

(1)Center for Low-Emission Transport, AIT Austrian Institute of Technology, Austria, martin.czuka@ait.ac.at

(2)Institute of Electronic Music and Acoustics (IEM), University of Music and Performing Arts Graz, Austria

ABSTRACT

When encountering a physical object that occludes its inner structure or content, we often resort to a tried and tested remedy: hit and listen. The resulting auditory feedback conveys information on the physical properties of the involved objects (e.g., material and geometry) and the performed action. For the interpretation of such auditory feedback, we need to evaluate the inverse of a physical model that describes the relationship between object, action, and sound. As the inverse system is underdetermined, a Bayesian interpretation of probability based on plausible combinations of physical parameters is required. Robotic perception of physical properties might benefit from incorporating models of the underlying physical processes in conjunction with application-specific probabilities. Here we introduce a model-based algorithm for estimating geometry and material of rectangular plates by sound. In direct comparison with untrained human listeners, it achieves superior identification performance when judging aspect ratio and material from impact sounds. The results demonstrate the benefit of model-based robotic perception for practical applications such as non-destructive inspection or handling of hazardous waste. In addition, the proposed algorithm helps us to understand how physical information is encoded in the sound of rectangular plates, and how it is extracted by human listeners.

Keywords: Sound in multisensory perception and interactions, Psychoacoustics

1 INTRODUCTION

In everyday life, humans are often able to distinguish and identify physical objects based on their sound. For example, we tap on melons to estimate their degree of ripeness, or shake the coffee can to determine its filling level. Before entering the office kitchen where our coffee can resides, we knock at the door so that our colleagues are acoustically informed beforehand. The radiated sound caused by the interaction with solid objects like a door is characterized by the objects' shape, size and material properties, as well as by the type of excitation. The distinction between sounds as well as their interpretation in our acoustic environments happens on a daily basis, and often unconsciously. If acoustic feedback is caused by our own interaction with a physical object, as depicted in Figure 1, we refer to it as auditory feedback.

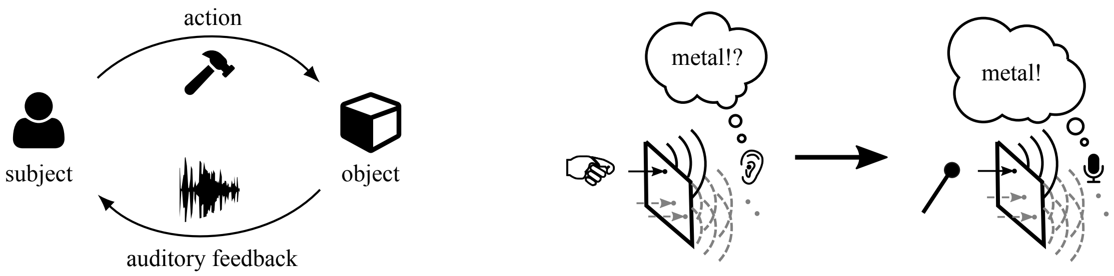

Figure 1. Interaction loop with auditory feedback (left) and schematic scenario from human to robotic acoustic characterization of rectangular plates (right).

The acoustic distinction and characterization of basic physical objects by humans was already investigated in a wide range of studies (e.g., [1, 2, 3, 4, 5, 6]). In [1], participants of a listening experiment rated how well sounds of struck cylinders conveyed that they were made of a certain material. While the participants could clearly identify the gross material classes metal-glass and wood-plastic, separating materials within each group was ambiguous. The inability to consistently discriminate between materials with similar longitudinal bending wave velocity (e.g., glass and aluminum) was also found in [2] with sounds of rectangular plates, and in [3] with real and synthesized rigid-body contact sounds.

The extraction of information about physical objects from a sound is an ability not unique to living beings. By employing algorithms based on physical or machine-learning models, computers are able to conclude on material-inherent objects properties. Fundamental work on robotic perception of materials presented in [7] describes several strategies for acoustic characterization of physical objects; one of these being "hit and listen". More sophisticated methods demonstrate several fields of application based on this objective. In [8] and [9], physical-model-based computational procedures were used for material quality inspection of bars and plates. Within the field of handling and recycling of waste, a procedure presented in [10] offers the potential to sort waste not only by visual but also by acoustic cues. In [11], the vibrational behavior of a waste bin was monitored to automatically detect its filling level.

Within this work, we introduce an algorithm for estimating the geometry and the material of rectangular plates by sound. As visualized in Figure 1, the method is able to extract basic information from sounds of impacted plates analogously to the human auditory system. The method is based on well-established physical models (described, e.g., in [12]) of thin plates and builds upon available knowledge on the acoustic perception of simple-shaped objects such as plates and bars. Furthermore, a modal synthesis model introduced in [13] with a comprehensive damping model from [14] was used to create sounds for impacted rectangular plates of different sizes and materials. The synthesized sounds were employed in an listening experiment to investigate the perceptibility of these physical object properties. In this work we discuss and compare the results of the listening experiment with the results of the robotic characterization of the proposed algorithm. The algorithm is based deliberately on physical models rather than readily available machine learning algorithms, since we wonder what performance a detection method of this kind is able to achieve.

2 ALGORITHMIC CHARACTERIZATION METHOD

For the developed algorithm to estimate the geometry and the material of a rectangular plate, we assume a detection scenario as depicted in Figure 1. A situation in which a human would try to detect the properties of a physical object by ear would consist of tapping, knocking and scratching at multiple positions while listening to the emitted sounds of the object. In order to mimic this situation in a simplified and reproducible way, we assume a plate sound caused by impacts of a simple mallet, recorded in the vicinity of the plate. We expect the microphone recording $s(t)$ of a single impact to be decomposable into

$$s(t) = \sum_{m=1}^{M} A_m \sin(\omega_m t + \phi_m) e^{-\alpha_m t}. \quad (1)$$

Each sinusoid describes a plate mode m with the angular eigenfrequency $\omega_m = 2\pi f_m$ that subsides with the decay factor α_m over time t. The underlying plate to characterize is also described by its thickness h, area $A = L_x L_y$ (with dimensions L_x and L_y in x- and y-direction, respectively), the material properties density ρ, Young's modulus E, Poisson's ratio ν and the loss factor $\eta_m = 2\alpha_m/\omega$. In addition, we define the aspect ratio of the plate with $r_a = \min\{L_x, L_y\}/\max\{L_x, L_y\} \leq 1$. In its current version, the characterization algorithm attempts to estimate the parameters of an isotropic material.

A schematic overview of the developed method is depicted in Figure 2. The first part comprises the extraction of the parameters f_m and α_m, which subsequently serve as basis for two procedures - a decay factor regression to estimate a material-inherent loss factor, and a steepest descent algorithm to fit the eigenfrequencies to a model plate with specific dimensions and material properties. In addition, a decay factor spectrum is determined to calculate the critical radiation frequency f_{crit}. All this extracted information is then utilized to estimate the geometry and material of a plate that fits best (in terms of the metrics of the algorithm) to the

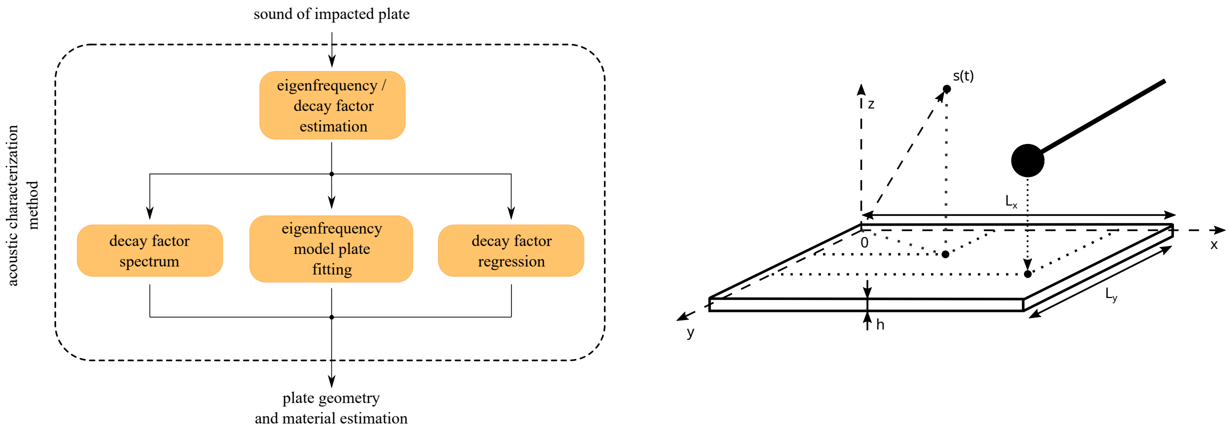

Figure 2. Overview of the acoustic characterization method (left) and geometric setup for synthesized plate sounds (right).

provided plate sound. Since the inverse system is underdetermined, we know that there is no unique solution to our task. However, not every combination of parameters that represents a solution is actually physically feasible. By focusing on materials, which are useful for the construction of plates (e.g., metals, wood, or plastics), the theoretically infinite value ranges for material parameters become limited. Furthermore, we may consider current limitations of manufacturing processes. For instance, the production of glass plates at larger thicknesses is extremely difficult without cracking due to the occurring thermal stress in the casting process.

2.1 Determination of eigenfrequencies and decay factors

In order to extract the plate eigenfrequencies f_m and decay factors α_m as part of the signal model from Equation 1, we identify and track the most prominent spectral peaks in the given signal. This is a frequently encountered task in a wide range of applications, such as in speech processing and synthesis [15], digital audio signal processing in musical applications [16], or vehicle engine order tracking [17]. For the acoustic characterization, the fast partial tracking algorithm presented in [18] is employed. While several algorithms are suited for the given task, this particular method was selected due to its availability and its presented robust performance. The underlying signal model assumes time-varying amplitudes, frequencies and phases for each detected partial. The parameters of every partial are determined for every analysis frame of the short-term Fourier transform (STFT) of the input signal. In order to allow arbitrary changes in frequency over time, including crossing partials, the detected partials of the individual analysis frames are connected by solving a linear assignment problem. Figure 3 visualizes the application of the partial tracking algorithm on an exemplary sound of an impacted rectangular plate with free edges.

The most prominent detected partials above a lower frequency threshold (e.g., 50 Hz to neglect possible low-frequency noise) are selected for further processing. In order to obtain the eigenfrequencies f_m for our initial signal model in Equation 1, a time-averaged frequency is computed for every selected partial. If the standard deviation of the time-varying partial frequency exceeds a selected threshold, the partial is withdrawn since our signal model requires an (almost) constant frequency. The decay factors α_m are computed from the temporal decay of the amplitudes of the partials. By assuming an ideal exponential decay of the form $A_m e^{-\alpha_m t}$, a linear regression can be computed from the logarithm of the amplitudes to estimate the decay factors α_m and the weighting factors A_m. If the applied linear regression has a Pearson correlation coefficient larger than a selected limit value (e.g., -0.9), we assume that the partial does not decay exponentially, as required by our model. Hence, partials that exceed this limit value are withdrawn. Furthermore, partials with estimated decay factors, that are implausibly small or large for a specific frequency region, are not used for the signal model. Figure 3 shows the extracted model parameters f_m and α_m from the sound of an exemplary impacted plate with free edges. Additional case studies for the estimation of the signal model parameters using the original version of the acoustic characterization method are part of [19], Section 4.1.

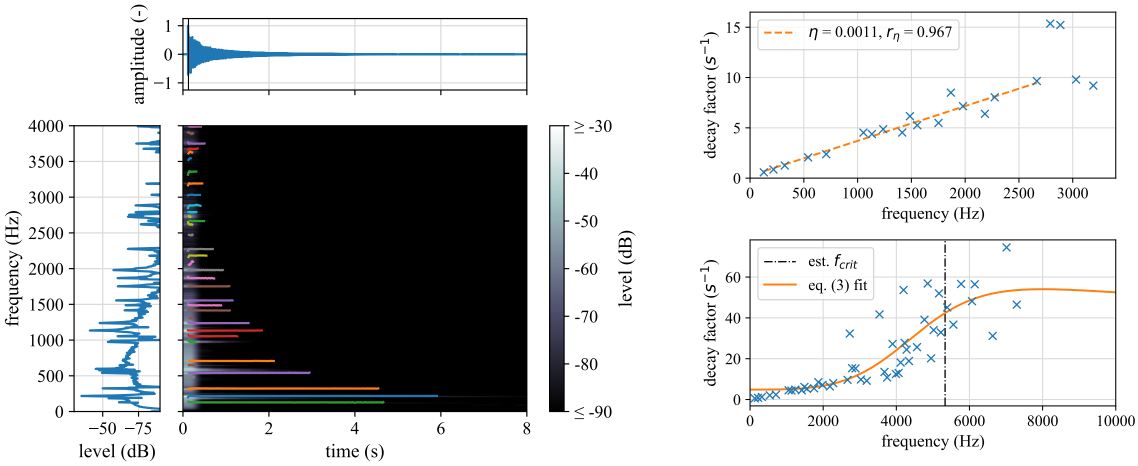

Figure 3. Partial tracking (left) and extracted model parameters f_m, α_m, f_{crit} and η (right) from a recorded sound of an exemplary rectangular glass plate with free edges.

2.2 Estimation of plate properties

As a result from the previous analysis steps we now possess parameters for the signal model introduced in Equation 1. Based on a set of eigenfrequencies f_m with their associated decay factors α_m, we are able to derive physical properties from the sound of the impacted rectangular plate. The critical radiation frequency

$$f_{crit} = \sqrt{3}\frac{c_{air}^2}{\pi h c_L} \qquad \text{with} \qquad c_L = \sqrt{\frac{E}{\rho(1-\nu^2)}} \tag{2}$$

of an isotropic plate represents the first auxiliary quantity that is estimated from our signal model. Below this critical frequency, the radiation efficiency is weak and consequently the decay factors α_m of the plate modes in this region are small. On the other hand, modes with eigenfrequencies above f_{crit} decay fast. This behavior is considered in the plate damping model presented in [14] via radiation damping. Besides, the damping law also considers viscoelastic, thermoelastic and viscous losses. In order to estimate f_{crit} from our given signal model, we use an empirical formula in [6] for this plate damping law and extend it by a constant p_0 to

$$\alpha(f) = \frac{p_a f^3}{f^3 - p_b f + \frac{2}{3} p_b f_c} + p_0 \tag{3}$$

to model the decay factor spectrum with our extracted α_m. The modeling is achieved with a nonlinear least squares fit, which is exemplarily visualized in Figure 3 for a glass plate. For the investigated plate sounds in this work, the frequency $f = \frac{2}{3} f_c$, where the decay factor in Equation 3 diminishes to $\alpha = p_a + p_0$, provides a good estimate for f_{crit}.

Since below f_{crit} the decay factors tend to be dominated by internal damping behavior of the material, we assume that a constant loss factor $\eta = \frac{\alpha}{\pi f}$ serves as a robust predictor of the material-inherent damping in this frequency region. Laser vibrometer measurements of the decay factor performed in [14, 19] indicate an almost linear relation between eigenfrequency and decay factor for viscoelastic damping in glass. If thermoelastic damping dominates, the linear increase is superimposed by the varying influence of the plate mode shapes. In any case, we apply a linear regression on the extracted decay factors α_m below f_{crit} to find values for η and α_0 in the model

$$\alpha(f) = \eta \pi f + \alpha_0. \tag{4}$$

The corresponding Pearson correlation coefficient r_η provides hints on the kind of damping that is dominant in the material. Values significantly smaller than 1 in conjunction with a loss factor smaller than 10^{-3} may indicate materials with dominant thermoelastic damping, as with metals. Figure 4 illustrates typical value ranges of loss factors for different materials.

The third analysis for the acoustic characterization method does not utilize decay factors, but the extracted eigenfrequencies from the plate sound. Assuming an isotropic plate, the simplified frequency formula introduced in [20] can be rearranged to

$$f = \Phi\sqrt{G_x^4\frac{1}{r_a^2} + G_y^4 r_a^2 + 2\nu H_x H_y + 2(1-\nu)J_x J_y} \qquad \text{with} \qquad \Phi = \frac{\pi}{\sqrt{48}}\frac{hc_L}{A}, \tag{5}$$

where the coefficients G, H, and J depend on the boundary conditions and the plate mode numbers. Poisson's ratio is initially assumed as constant with ν = 0.35, since this value seems to be a reasonable well approximation for most materials ([12], p. 590). The aim is now to determine values for Φ and the aspect ratio r_a, which lead to frequencies that best fit a limited number of extracted frequencies f_m from the plate sound. These frequencies represent a subset of estimates $\tilde{f}_i$ for the theoretical infinite number of model plate eigenfrequencies f_j. However, some low modes may be missing due to weak radiation efficiency or because of destructive interferences at the observation point. Therefore, every extracted $\tilde{f}_i$ gets exclusively assigned to a model eigenfrequency f_j by solving a linear assignment problem

$$\min\left\{\sum_{i=1}^{I}\sum_{j=1}^{J} C_{ij}X_{ij}\right\} \quad \text{with} \quad \sum_{i=1}^{I} X_{ij} = 1, \qquad \sum_{j=1}^{J} X_{ij} = 1 \quad \text{and} \quad C_{ij} = \frac{|\tilde{f}_i - f_j[k]|}{\tilde{f}_i}. \tag{6}$$

The matrix $\mathbf{X}$ represents a binary matrix only containing the non-zero value 1 for assignments between extracted and model eigenfrequencies. The elements C_{ij} of the cost matrix $\mathbf{C}$ specify the costs of every possible assignment. In order to find suitable values for Φ and r_a, a steepest descent algorithm is applied with a set of initial values at k = 0. In each iteration step k the value pair of the model plates is updated according to

$$\Phi[k+1] = \Phi[k] - \mu_\Phi \frac{\partial \min\left\{\sum_I \sum_J C_{ij}X_{ij}\right\}}{\partial \Phi} \quad \text{and} \quad r_a[k+1] = r_a[k] - \mu_{r_a} \frac{\partial \min\left\{\sum_I \sum_J C_{ij}X_{ij}\right\}}{\partial r_a}, \tag{7}$$

where μ_Φ and μ_{r_a} are the associated learning rates. By applying the steepest descent algorithm on a restricted grid of value pairs for Φ and r_a as initial values, each run converges to a local minimum on the assignment cost surface, as exemplary depicted in Figure 4. We argue now that accumulation points of local minima on the cost surface with small overall assignment costs represent suitable model plates with value pairs of Φ and r_a for our plate sound. In conjunction with our computed critical radiation frequency, an estimation of the plate area $A = L_x L_y$ and the product hc_L can be obtained via

$$A = \frac{c_{air}^2}{4 f_{crit}\Phi}, \qquad L_x = \sqrt{A r_a}, \qquad L_y = \sqrt{A/r_a} \quad \text{and} \quad hc_L = \frac{\sqrt{48}}{\pi}\Phi A. \tag{8}$$

Demonstration examples for the application of the algorithm in its initial version (which only slightly differs in the estimation procedures for f_{crit} and α_m) can be found in [19], Section 4.3.

3 ROBOTIC AND HUMAN PERCEPTION OF PLATE PROPERTIES

In order to validate the proposed acoustic characterization algorithm with a larger set of plate sounds, we employed the algorithm to classify stimuli that were created for a listening experiment described in [13]. The experiment was originally designed to investigate the auditory discrimination of material and aspect ratio of rectangular plates within [21]. By confronting the characterization algorithm with the same set of possible answers as the human listeners within this work, we are able to directly compare between human and robotic acoustic characterization performance.

Within the listening experiment conducted in [21], every participant had to assign three plate properties to each presented plate sound from sets of discrete possible answers: metallicity (non-metal / metal), material

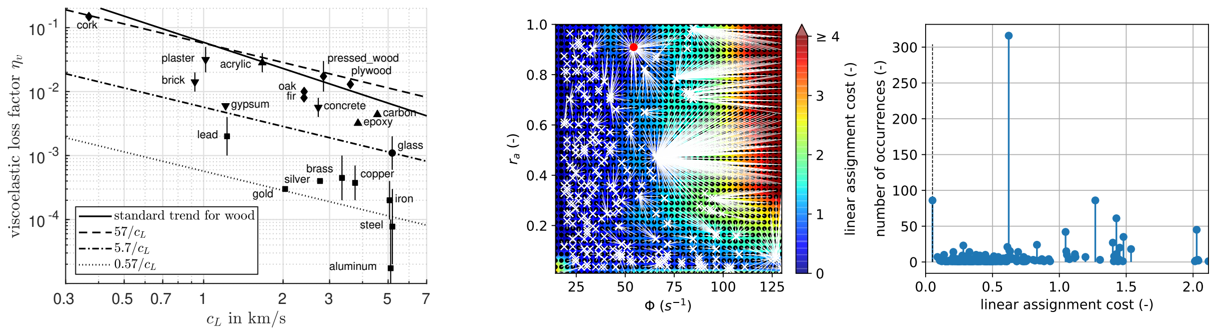

Figure 4. Loss factor η as a function of longitudinal wave velocity c_L from [13], Section 3.2.6 (left); cost function (center) with true values (red dot) and paths of the gradient search (white lines) and assignment cost histogram (right) with best fit (dashed line) for a synthesized sound of an exemplary aluminum plate (right).

(plastic / wood / glass in case of non-metals, gold / brass / aluminum for metals), and aspect ratio (0.5 / 0.25 / 0.125). The stimuli comprise a series of rendered plate sounds using modal synthesis. The plate eigenfrequencies were computed from the quotients between potential and kinetic energy caused by the transverse displacement of the plate bending wave of the corresponding plate modes ($\omega^2 = \frac{E_{pot}}{E_{kin}}$). Simple mode shapes for a plate with free edges proposed in [20] were employed for the eigenfrequency calculation as well as for the decay factor computation according to [14]. Additional damping was introduced to create plausible overall decay times between T_{60} = 0.15 s and T_{60} = 0.45 s with a constant bias to the decay factors. We argue that almost any frequency-dependent damping higher than that of the ideal free plate freely hovering in the air can be achieved by some kind of physical suspension. In order to take the acoustic shortcut between front and back surface of the unbaffled plate into account, the empirical formula for the average radiation efficiency presented in [22] was applied through an individual gain for each mode. Table 5.12 in [13] lists the employed model coefficients to render the plate sounds. The experiment was implemented in form of a web page, with the help of the open-source JavaScript library jsPsych. A more detailed explanation of the used models for the plate sound renderings as well as of the listening experiment can be found in [13].

By default, the proposed acoustic characterization algorithm in this work outputs estimates of the following plate properties: aspect ratio r_a, area $A = L_x L_y$, critical radiation frequency f_{crit}, loss factor η, as well as the product of plate thickness and longitudinal wave velocity hc_L. In order to provide the same kind of classifications as offered as in the listening experiment, we derived a set of predictors. Based on our observations in Section 2.2 we classify the gross material category as metal if the following two criteria are met: $\eta < 10^{-3}$ and $r_\eta < 0.9$. Otherwise, a non-metallic material is assumed. A reliable predictor for the material within each gross category for the listening experiment stimuli turned out to be the statistical distribution of f_{crit}, due to its dependence on hc_L. Since it is known that a bar-shaped plate has a lower modal density than a plate with an aspect ratio close to 1 (see, e.g., [19]), we can argue that the combined effect of the radiation damping above f_{crit} and the low-pass characteristics of a typical impact force (e.g., caused by a mallet strike) leads to less detected eigenfrequencies by our partial tracking algorithm. Therefore we use the quotient M/f_{crit}^n, with M being the total number of detected eigenfrequencies for our signal model in Equation 1, as metric for aspect ratio classification. With the chosen control parameters for the partial tracking algorithm and the exponent n = 0.5, the values 0.48 and 0.65 served as selection boundaries between the aspect ratios 0.125, 0.25 and 0.5 for the listening experiment stimuli. Finally, accuracies for correctly classified aspect ratios, material categories and materials were computed. The comparisons between robotic characterization and average listening experiment results in Figure 5 show, that the algorithm is slightly superior in identifying the material category (accuracy of 0.85 compared to 0.80, labeled as metallicity). The algorithm is significantly more accurate in classifying the material within each material category (accuracy of 0.74 compared to 0.55, labeled as rigidity) as well as in selecting the correct aspect ratio (accuracy of 0.76 compared to 0.36). Furthermore, the results prove that the algorithm is able to make useful classifications based on plate sounds with short decay times T_{60} of 0.15 s.

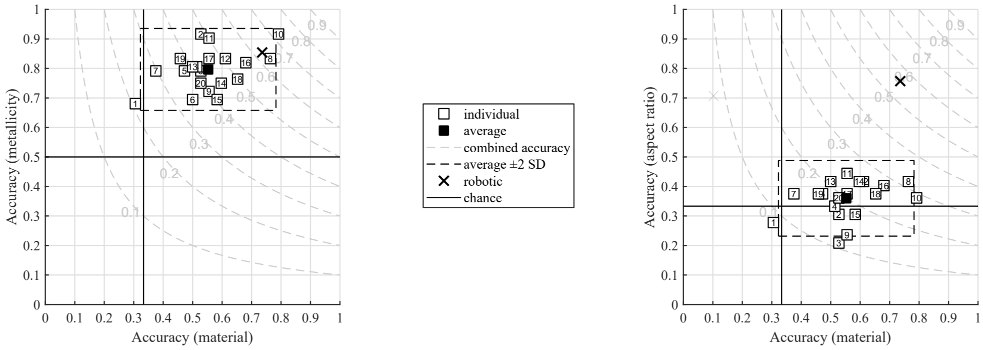

Figure 5. Individual participants' accuracies together with their average and robotic results.

4 CONCLUSIONS AND FUTURE WORK

In this work we proposed a novel method to conclude on the physical properties of a plate by sound. Based on extracted eigenfrequencies and decay factors as part of a simple signal model of exponentially decaying sinusoids, we are able to estimate a material-inherent loss factor and the critical radiation frequency of the plate. By assuming an isotropic rectangular plate, the method is capable of estimating the size of model plates whose eigenfrequencies approximately fit to the extracted frequencies of the provided plate sound. In direct comparison with untrained listeners, we demonstrated that on average the algorithm is able to conclude on the actual aspect ratio and material of simulated plates with superior accuracy. As with the human auditory system, the algorithm prerequisites plate sounds with at least short decay times in order to make meaningful estimations.

In its current version, the acoustic characterization method assumes an isotropic rectangular plate with ideal boundary conditions to estimate its size. The performance of the required model plate fitting to estimate the size depends on the accuracy of the extracted plate eigenfrequencies as well as on the design of the linear assignment cost matrix. Furthermore, with the employed analyses and models we are not yet able to separate between plate thickness and longitudinal wave velocity of the bending waves. Future work may address the overcome of these issues and limitations to increase the practical applicability of the characterization algorithm. The software code that fully implements the acoustic characterization method is available at https://gitlab.com/helmholtz86/acoucharacterize_plates.

ACKNOWLEDGMENTS

The initial version of the acoustic characterization method presented here was originally developed in [19] and summarized in [23] as well as in [13]. All listening experiments described in this work were conducted within [21]. Comprehensive research on the interaction with physical objects in acoustic environments and their auditory augmentation was carried out in [13].

REFERENCES

[1] Lemaitre G, Heller LM. Auditory perception of material is fragile while action is strikingly robust. The Journal of the Acoustical Society of America. 2012;131(2):1337-48.

[2] Giordano BL, McAdams S. Material identification of real impact sounds: Effects of size variation in steel, glass, wood, and plexiglass plates. The Journal of the Acoustical Society of America. 2006;119:1171-81.

[3] Traer J, Cusimano M, McDermott JH. A perceptually inspired generative model of rigid-body contact. In: Proceedings of the 22nd International Conference on Digital Audio Effects. Birmingham, UK; 2019. p. 136-43.

[4] Klatzky RL, Pai DK, Krotkov EP. Perception of Material from Contact Sounds. Teleoperators and Virtual Environments. 2000;9(4):399-410.

[5] McAdams S, Chaigne A, Roussarie V. The psychomechanics of simulated sound sources: Material properties of impacted bars. The Journal of the Acoustical Society of America. 2004;115(3):1306-20.

[6] McAdams S, Roussarie V, Chaigne A, Giordano BL. The psychomechanics of simulated sound sources: Material properties of impacted thin plates. The Journal of the Acoustical Society of America. 2010;128:1401-13.

[7] Krotkov E. Robotic Perception of Material. In: Proceedings of 14th International Joint Conference on Artificial Intelligence; 1995. p. 88-94.

[8] McIntyre ME, Woodhouse J. On Measuring the Elastic and Damping Constants for orthotropic Sheet Materials. Acta Metallurgica. 1988;35(6):1397-416.

[9] Muravyev VV, Muravyeva OV, Kokorina EN. Quality Control of Heat Treatment of 60C2A Steel Bars Using the Electromagnetic–Acoustic Method. Russian Journal of Nondestructive Testing. 2013;49(1):15-25.

[10] Huang J, Pretz T. Feasibility of Acoustic Sorting for Black Materials in Solid Waste Processing. In: Waste-to-Resources; 2009. p. 439-58.

[11] Zhao Y, Yao S, Li S, Hu S, Shao H, Abdelzaher TF. VibeBin: A Vibration-Based Waste Bin Level Detection System. Proceedings of the ACM on Interactive, Mobile, Wearable and Ubiquitous Technologies. 2017;1(3):1-22.

[12] Rossing TD. Springer Handbook of Acoustics. 2nd ed. Springer Verlag; 2014.

[13] Weger M. Plausible auditory augmentation of physical interaction [PhD thesis]. Graz: University of Music and Performing Arts Graz; 2022.

[14] Chaigne A, Lambourg C. Time-domain simulation of damped impacted plates. I. Theory and experiments. The Journal of the Acoustical Society of America. 2001;109(4):1422-32.

[15] McAulay RJ, Quatieri TF. Speech Analysis / Synthesis Based on a Sinusoidal Representation. IEEE Transactions on Acoustics, Speech, and Signal Processing. 1986;34(4):744-54.

[16] Lagrange M, Marchand S, Rault JB. Tracking Partials for the sinusoidal Modeling of polyphonic Sounds. In: IEEE Transactions on Acoustics, Speech, and Signal Processing. vol. 3; 2005. p. 229-32.

[17] Czuka M. Development of an analysis method for the extraction of sound synthesis parameters from driving noise of motor vehicles [Student project]. Graz: University of Music and Performing Arts Graz; 2014.

[18] Neri J, Depalle P. Fast Partial Tracking of Audio with real-time Capability trough linear programming. In: roceedings of the 21st International Conference on Digital Audio Effects. Aveiro, Portugal; 2018. p. 326 333. Available from: www.github.com/jundsp/Fast-Partial-Tracking.

[19] Czuka M. Sound Synthesis and Acoustic Characterization of Rectangular Plates [Diploma thesis]. Graz: University of Music and Performing Arts Graz; 2021.

[20] Warburton GB. The Vibration of Rectangular Plates. Proceedings of the Institution of Mechanical Engineers. 1954;168(1):371-84.

[21] Aurenhammer MB. Informationsgehalt rechteckiger Platten [Bachelor's thesis]. Graz: University of Music and Performing Arts Graz; 2021.

[22] Putra A, Thompson DJ. Sound radiation from rectangular baffled and unbaffled plates. Applied Acoustics. 2010;71(12):1113-25.

[23] Czuka M, Weger M, Höldrich R. Klangsynthese und akustische Erkennung rechteckiger Platten. In: Proceedings of the 47th Jahrestagung für Akustik. Vienna, Austria; 2021. p. 667-70.